

Internal Wasserstein Distance for Adversarial Attack and Defense

Jincheng Li^{*1} Jiezhong Cao^{*2} Shuhai Zhang¹ Yanwu Xu³ Jian Chen¹ Mingkui Tan^{1,4}

Abstract

Deep neural networks (DNNs) are vulnerable to adversarial examples that can trigger misclassification of DNNs but may be imperceptible to human perception. Adversarial attack has been an important way to evaluate the robustness of DNNs. Existing attack methods on the construction of adversarial examples use such ℓ_p distance as a similarity metric to perturb samples. However, this kind of metric is incompatible with the underlying real-world image formation and human visual perception. In this paper, we first propose an internal Wasserstein distance (IWD) to measure image similarity between a sample and its adversarial example. We apply IWD to perform adversarial attack and defense. Specifically, we develop a novel attack method by capturing the distribution of patches in original samples. In this case, our approach is able to generate semantically similar but diverse adversarial examples that are more difficult to defend by existing defense methods. Relying on IWD, we also build a new defense method that seeks to learn robust models to defend against unseen adversarial examples. We provide both thorough theoretical and empirical evidence to support our methods.

1. Introduction

Deep neural networks (DNNs) are vulnerable to adversarial examples (Szegedy et al., 2014; Dai et al., 2018; Zhao et al., 2018; Xu et al., 2019; Croce & Hein, 2020) mainly due to their overfitting nature (Rice et al., 2020). Particularly, this issue becomes more severe if we have only limited training data for a specific task. In fact, the neural network tends to fit the training data well and may make an incorrect prediction for an example contaminated by only slight perturbations or transformations. However, the security of deep learning

^{*}Equal contribution ¹South China University of Technology ²ETH Zürich ³Baidu Inc. ⁴Key Laboratory of Big Data and Intelligent Robot, Ministry of Education. Correspondence to: Mingkui Tan <mingkuitan@scut.edu.cn>.

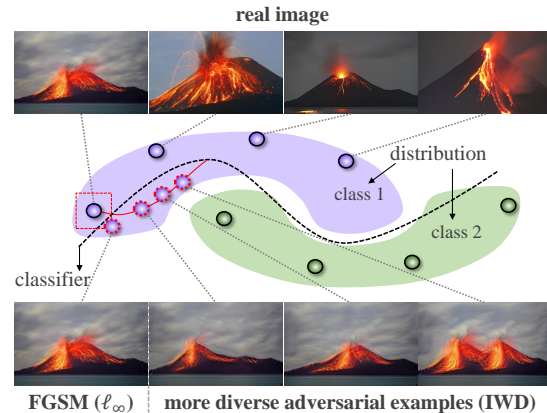


Figure 1. Illustration of different adversarial examples. Given a pre-trained classifier, we perturb a real image to generate semantically similar but diverse adversarial examples, relying on IWD instead of the ℓ_p distance (e.g., FGSM with the ℓ_∞ perturbation).

systems is vulnerable to crafted adversarial examples, which may be imperceptible to the human perception, but can lead the model to misclassify the output (Ronneberger et al., 2015). In practice, adversarial examples can be crafted by perturbing or transforming some image pixel values to ensure they “look like” the original images. Such “look like” is a perceptual metric that can be defined in the Euclidean space, which, however, suffers from two limitations.

First, most attack methods (Goodfellow et al., 2014; Madry et al., 2018; Pang et al., 2018) use the ℓ_p distance as a similarity metric which is inconsistent with the underlying real-world image formation and human visual perception. This metric is insensitive to human perceptual understanding (Larsen et al., 2016). For example, humans find it difficult to find the subtle difference when some sufficiently small pixel values of an image are changed. Moreover, the pixel-based transformations (e.g., perturbation or distortion) use this metric to ensure that adversarial examples are bounded in a small norm box. However, due to the slight perturbation, it is difficult for each image to find an effective adversarial example that causes misclassification of the classifier. More critically, a small image translation by changing some pixels may result in a large pixel-wise error whereas a human would barely discover the change. Therefore, how to measure the similarity of a sample and its adversarial example in attack methods is very necessary and important.

Second, attack methods using the ℓ_p distance understand an input image from a one-sided view in Euclidean space and may be insufficient to perturb samples on a low-dimensional manifold. Thus, the crafted adversarial examples may lack sufficient diversity. Perturbing a sample on the manifold would obtain more diverse and valuable adversarial examples since high-dimensional data often lie on some low-dimensional manifold (Tenenbaum et al., 2000; Roweis & Saul, 2000). In this sense, it has great practical value to design this type of attack. Moreover, these attack samples can help in covering the blind area of the data distribution to develop robust models, which can well describe the boundaries of different classes with a large margin. Unfortunately, how to generate diverse adversarial examples and build robust models with the help of them is unknown.

In this paper, we investigate two key questions: 1) how to effectively attack a model on the manifold; and 2) how to build robust models relying on those attacks. Nevertheless, we find the commonly used ℓ_p distance is insufficient when conducting attack and defense to DNNs on the manifold. To address this, we propose an internal Wasserstein distance (IWD). Relying on IWD, we develop a new attack method (called IWDA) to perturb samples on the manifold. Correspondingly, we develop a defense method (called IWDD) to defend against unseen adversarial examples.

The contributions of this paper are summarized as follows:

- We analyze why the ℓ_p distance is insufficient when doing attack and defense to DNNs. We thus propose an internal Wasserstein distance (IWD) to exploit the internal distribution of data for both attack and defense tasks.
- We propose a novel attack method to generate diverse adversarial examples based on the distribution perturbation instead of the pixel perturbation. Additionally, we develop a new defense method to improve the robustness of the classifier. Experiments demonstrate the effectiveness of the proposed attack and defense methods.
- We analyze the generalization ability of the proposed defense method. Theoretical and empirical evidence justifies that the adversarial examples with more diversity are required in adversarial training.

2. Related Work

2.1. Adversarial Attack

Attack with the ℓ_p perturbation. Deep neural networks are vulnerable to adversarial examples with a certain hardly perceptible perturbation (Szegedy et al., 2014). Most existing methods (Goodfellow et al., 2014; Athalye et al., 2018; Croce & Hein, 2020) attempt to craft adversarial examples with the ℓ_p perturbation. However, the generated adversarial

examples cannot result in a large perturbation that can guarantee successful attacks. Moreover, the ℓ_p perturbation is not a good metric of image similarity (Alaifari et al., 2019).

Attack without the ℓ_p perturbation. To mitigate the limitations of the ℓ_p perturbations, several methods propose to generate adversarial examples with other perturbation norms. Specifically, Xiao et al. (2018) propose spatial transformations instead of pixel perturbation to generate adversarial examples. Zhao et al. (2018) apply generative adversarial networks to generate natural and legible adversarial examples that lie on a data manifold. In addition, Liu et al. (2019) introduce parametric norm-balls as an evaluation metric by perturbing physical parameters that produce image formations. Alaifari et al. (2019) propose the ADef algorithm to craft adversarial examples by applying small deformations to images iteratively. However, these crafted adversarial examples may lack diversity. In this paper, we propose a novel metric, internal Wasserstein distance (IWD), to generate diverse adversarial examples.

2.2. Adversarial Defense

To address the vulnerability of deep neural networks, many defense methods have been proposed to defend against adversarial examples. Recently, Goodfellow et al. (2014) propose an adversarial training method based on a fast gradient sign method, which demonstrates the effectiveness of adversarial training. However, the method is too weak to defend against other multi-step attack methods. Thus, Madry et al. (2018) present a robust defense method based on a projected gradient descent (PGD) method to improve the resistance of the model to a wide range of adversarial attacks. Unfortunately, training with PGD is time-consuming and computationally intensive because it generates adversarial examples with multi-step updates. To address this, free-PGD (Shafahi et al., 2019) speeds up the training and improves the robustness of the model. Besides, Kannan et al. (2018) propose to encourage logits for example pairs to be similar and maintain good accuracy on clean examples.

Recently, PGD adversarial training is still a popular method to defend against adversarial examples. However, most studies (Tsipras et al., 2019; Raghunathan et al., 2020; Yang et al., 2020) posit that a robustness-accuracy trade-off may be inevitable in PGD adversarial training method. To this end, TRADES (Zhang et al., 2019) proposes a differentiable upper bound to trade adversarial robustness off against accuracy. Moreover, FAT (Zhang et al., 2020) applies early stopping to craft adversarial examples to make these adversarial training methods stronger. However, these methods are limited in improving the robustness of a classifier due to the limitations of the ℓ_p distance. In this paper, we apply IWD to perform defense methods and derive an upper bound to enhance the robustness.

3. Notation and Motivations

Notation. We use calligraphic letters (e.g., \mathcal{X}) to denote spaces, and bold lower case letters (e.g., \mathbf{x}) to denote vectors. Without loss of generality, we consider a multi-class classification problem. Let \mathcal{D} be the real data distribution, and $\mathcal{D}_n = \{\mathbf{x}_i, \mathbf{y}_i\}_{i=1}^n \in \mathcal{X} \times \mathcal{Y}$ be the training data, where \mathcal{X} and \mathcal{Y} denote the data and label space, respectively. We denote by $h : \mathcal{X} \rightarrow \mathcal{Y}$ a classifier learned on \mathcal{D}_n . Let $\text{diam}(\mathcal{A})$ be the diameter of a set \mathcal{A} and $\delta_{\mathbf{x}}$ be the Dirac distribution at a point \mathbf{x} . We use $\mathbb{1}\{A\}$ to represent an indicator function, where $\mathbb{1}\{A\} = 1$ if A is true and $\mathbb{1}\{A\} = 0$ if A is false. Let $\epsilon(d)$ be a sufficiently small constant with respect to some metric d , and $\mathcal{B}_{\mathbf{x}}(\mathbf{x}, \epsilon(d)) = \{\tilde{\mathbf{x}} \in \mathcal{X} \mid d(\mathbf{x}, \tilde{\mathbf{x}}) \leq \epsilon(d)\}$ be the $\epsilon(d)$ -neighborhood set of \mathbf{x} . Similarly, let $\mathcal{B}_h(h, \epsilon(d)) = \{\mathbf{x} \in \mathcal{X} \mid \exists \tilde{\mathbf{x}} \in \mathcal{B}_{\mathbf{x}}(\mathbf{x}, \epsilon(d)) \text{ s.t. } h(\mathbf{x}) \neq h(\tilde{\mathbf{x}})\}$ be the $\epsilon(d)$ -neighborhood set of h , as shown in Figure 2.

To begin with, we provide the definition of the adversarial example to develop our proposed method.

Definition 1 ($\epsilon(d)$ -adversarial example) *Given a sample pair (\mathbf{x}, \mathbf{y}) , the sample \mathbf{x} admits an $\epsilon(d)$ -adversarial example if there exists a sample $\tilde{\mathbf{x}} \in \mathcal{X}$ such that $h(\tilde{\mathbf{x}}) \neq \mathbf{y}$ and $d(\mathbf{x}, \tilde{\mathbf{x}}) \leq \epsilon(d)$, $\epsilon(d) > 0$.*

To construct an adversarial example $\tilde{\mathbf{x}}$, most existing methods (e.g., FGSM (Goodfellow et al., 2014)) impose some small transformation (e.g., perturbation) on \mathbf{x} . In particular, they use the ℓ_p distance as the metric d to measure a sample and its adversarial example. However, this metric is insufficient when conducting attack and defense to DNNs.

Limitation of the ℓ_p distance to attack. The attack methods using the ℓ_p distance are insufficient to deal with more general real-world cases. Specifically, the ℓ_p distance may only guarantee generating adversarial examples that are close to the original sample due to small perturbation, see Figure 1. If an original sample is far away from the decision boundary (described by a pre-trained classifier), it is hard for those samples to find the effective adversarial examples that can lead the pre-trained classifier to misclassify the output. Thus, the ℓ_p distance is insufficient to conduct adversarial attacks when a good classifier can well describe the boundaries of different classes with a large margin.

Limitation of the ℓ_p distance to defense. Most existing defense methods augment the training procedure by searching for adversarial examples relying on the ℓ_p distance. In this case, they try to cover the blind area of the data distribution and learn a good classifier, which can well describe the boundaries of different classes and can be robust to adversarial examples. However, they may fail to cover the whole data distribution due to the limited range of the ℓ_p perturbation, leading to inferior defense performance. To address this, we propose a new metric to exploit the internal distribution of data for both attack and defense tasks.

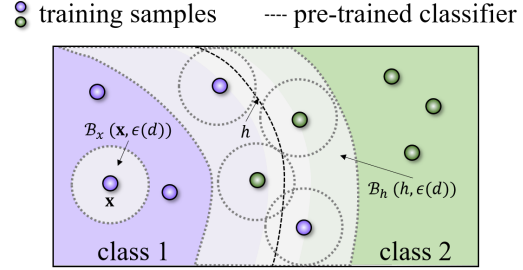


Figure 2. Illustration of notations.

3.1. Internal Wasserstein Distance

As aforementioned, the attack and defense methods relying on conventional metrics (e.g., the ℓ_p distance) are insufficient to perturb the distribution of samples on complex distributions. Recently, the Wasserstein distance (Villani, 2008) has been proposed to measure the differences between two any distributions and widely used in generated adversarial networks (GANs) (Arjovsky et al., 2017; Gulrajani et al., 2017).

Definition 2 (Wasserstein distance (Villani, 2008)) *Given two distributions \mathcal{D} and \mathcal{D}' , the Wasserstein distance can be defined as:*

$$\mathcal{W}(\mathcal{D}, \mathcal{D}') = \inf_{\mathbb{T} \in \Pi(\mathcal{D}, \mathcal{D}')} \mathbb{E}_{(\mathbf{x}, \mathbf{x}') \sim \mathbb{T}} [\|\mathbf{x} - \mathbf{x}'\|_1], \quad (1)$$

where $\mathbf{x} \sim \mathcal{D}$ and $\mathbf{x}' \sim \mathcal{D}'$. Here, Π is a set of all joint distributions \mathbb{T} whose marginal distributions are \mathcal{D} and \mathcal{D}' .

Note that while the Wasserstein distance has been widely used in GANs, it is non-trivial to apply it to conduct adversarial attack, since it may make the generated adversarial examples totally different from the original ones. To address this, we propose an internal Wasserstein distance (IWD) to measure the internal distribution distance between a sample \mathbf{x} and its adversarial sample $\tilde{\mathbf{x}}$. Specifically, let $\{\mathbf{u}_i\}_{i=1}^N$ and $\{\mathbf{v}_i\}_{i=1}^N$ be N patches drawn from two samples \mathbf{x} and $\tilde{\mathbf{x}}$, respectively. We define the internal distributions of \mathbf{x} and $\tilde{\mathbf{x}}$ as $\mu = \frac{1}{N} \sum_i \delta_{\mathbf{u}_i}$ and $\nu = \frac{1}{N} \sum_i \delta_{\mathbf{v}_i}$, respectively, where δ is the Dirac distribution (Alt, 2006). Then, we define the internal Wasserstein distance (IWD) as follows.

Definition 3 (Internal Wasserstein distance) *Given internal distributions μ and ν of \mathbf{x} and $\tilde{\mathbf{x}}$, respectively, the internal Wasserstein distance can be defined as:*

$$\mathcal{W}(\mathbf{x}, \tilde{\mathbf{x}}) := \inf_{\gamma \in \Gamma(\mu, \nu)} \mathbb{E}_{(\mathbf{u}, \mathbf{v}) \sim \gamma} [\|\mathbf{u} - \mathbf{v}\|_1], \quad (2)$$

where Γ is a set of all joint distributions γ whose marginal distributions are μ and ν .

Remark 1 *From the definition, the proposed IWD is different from the Wasserstein distance. Specifically, IWD measures the similarity between the distribution of patches in*

two images. In contrast, the Wasserstein distance measures the similarity between the distribution of two sets of images. In this sense, using the Wasserstein distance (e.g., WGAN (Arjovsky et al., 2017)) helps to generate significantly different image contents from original ones. This, however, can not be applied to conduct adversarial attack and defense.

From Definition 3, IWD captures the internal distributions of patches in original samples. In this sense, we are able to perturb a sample on the manifold when applying IWD as a metric to perform adversarial attack. Thus, this distribution perturbation can result in larger transformation than the pixel perturbation (e.g., the ℓ_p distance). To prove this, we provide the following theorem to compare two distances.

Theorem 1 Let $\epsilon(\ell_p)$ denote the perturbation relying on the ℓ_p distance. The perturbation $\epsilon(\mathcal{W})$ using the internal Wasserstein distance \mathcal{W} satisfies:

$$\text{diam}(\mathcal{B}_h(h, \epsilon(\ell_p))) \leq \text{diam}(\mathcal{B}_h(h, \epsilon(\mathcal{W}))).$$

Theorem 1 shows that the diameter of the neighborhood set \mathcal{B}_h in terms of $\epsilon(\mathcal{W})$ is larger than that in terms of $\epsilon(\ell_p)$. In other words, IWD obtain larger perturbation than the ℓ_p distance, i.e., $\epsilon(\ell_p) \leq \epsilon(\mathcal{W})$. Therefore, IWD would have a higher probability of finding valid adversarial examples that can cause model misclassification than the ℓ_p distance. In this paper, we apply IWD to perform adversarial attack and defense, as they can be considered as coupled tasks.

4. Adversarial Attack with IWD

In general, the **adversarial attack** aims to learn an adversarial attacker $g(\mathbf{x}, \mathbf{z})$ to confuse a classifier h , where \mathbf{z} can be a random noise vector or other kinds of input. In this paper, we consider two types of attacks, i.e., untargeted attack and targeted attack. Specifically, given a sample pair (\mathbf{x}, \mathbf{y}) , the untargeted attack aims to generate an adversarial example $\tilde{\mathbf{x}}$ such that $h(\tilde{\mathbf{x}}) \neq \mathbf{y}$. The targeted attack, however, aims to make the classifier classify $\tilde{\mathbf{x}}$ as the target label \mathbf{y}_t , i.e., $h(\tilde{\mathbf{x}}) = \mathbf{y}_t$, where $\mathbf{y}_t \neq \mathbf{y}$. Formally, both tasks can be formulated as the following optimization problems:

$$\underbrace{\max_g \mathcal{L}(h(\tilde{\mathbf{x}}), \mathbf{y})}_{\text{untargeted attack}} \quad \text{or} \quad \underbrace{\min_g \mathcal{L}(h(\tilde{\mathbf{x}}), \mathbf{y}_t)}_{\text{targeted attack}}, \quad (3)$$

where $\tilde{\mathbf{x}} = g(\mathbf{x}, \mathbf{z}) \in \mathcal{B}_x(\mathbf{x}, \epsilon(d))$, and $\mathcal{L}(\cdot, \cdot)$ is some loss function. In this case, the classifier h takes the adversarial examples as inputs and makes the wrong classification if the adversarial examples attack the classifier successfully.

Most existing methods mainly use the ℓ_p distance (e.g., ℓ_2 and ℓ_∞) to perturb a sample \mathbf{x} as an adversarial example $\tilde{\mathbf{x}}$. For example, FGSM (Goodfellow et al., 2014) uses the ℓ_∞ distance and the signed gradient vector \mathbf{z} ,

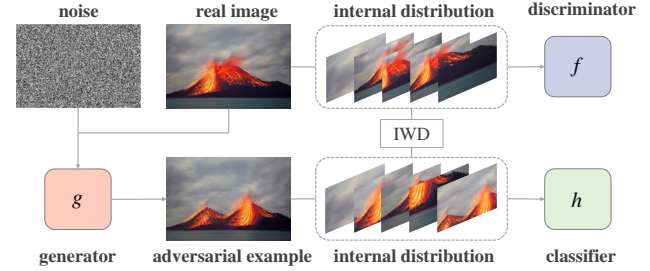


Figure 3. Illustration of our attack method (IWDA). Specifically, g produces an adversarial example such that f cannot distinguish the internal distribution of patches in the generated image from real data, i.e., the internal Wasserstein distance (IWD) between their internal distributions should be small. Then, h cannot correctly classify the generated adversarial examples. Note that the scales of patches are changed from small to large.

i.e., $g(\mathbf{x}, \mathbf{z}) = \mathbf{x} + \epsilon(\ell_\infty) \cdot \mathbf{z}$. However, these methods cannot guarantee successful attacks for every input due to the slight perturbations. From Theorem 1, our proposed IWD can obtain larger perturbations than the ℓ_p distance. Thus, we apply IWD to conduct adversarial attack to obtain diverse adversarial examples.

Relying on IWD, we are able to capture the internal distribution of patches in original examples and thus generate semantically similar but diverse adversarial examples. For example, the generated adversarial examples of a volcano image (see Figure 1) contain one or more volcanoes with different sizes, shapes and locations. These adversarial examples are new to the classifier and also different from the original image. In this sense, these adversarial examples are far away from the original image in the Euclidean space. However, it is non-trivial to directly apply IWD to perform adversarial attack to obtain such adversarial examples, since the infimum in Eqn. (2) is highly intractable (Arjovsky et al., 2017). To conduct adversarial attack with IWD, we next introduce the attack objective function.

4.1. Attack Objective Function

To generate $\epsilon(\mathcal{W})$ adversarial examples, we propose a new attack method relying on IWD, called IWDA. Figure 3 illustrates the overall scheme of IWDA. Specifically, we optimize an adversarial attack loss $\mathcal{L}_{\text{adv}}(f, g)$ to craft $\epsilon(\mathcal{W})$ -adversarial examples. Meanwhile, we optimize a classification loss $\mathcal{L}_c(g; h)$ such that the classifier misclassifies the adversarial examples. Then, the total objective function can be written as follows:

$$\mathcal{L}(f, g) = \mathcal{L}_{\text{adv}}(f, g) + \tau \mathcal{L}_c(g; h), \quad (4)$$

where τ is a hyper-parameter. Next, we introduce the adversarial attack loss and classification loss.

Adversarial attack loss. In Figure 3, the generator g aims to produce an adversarial example $\tilde{\mathbf{x}} = g(\mathbf{x}, \mathbf{z})$, and then the discriminator f distinguishes the internal distributions of patches in the adversarial example $\tilde{\mathbf{x}}$ and the original image \mathbf{x} . Relying on the internal Wasserstein distance, we propose to optimize the following adversarial loss:

$$\mathcal{L}_{\text{adv}}(f, g) = \max_{\|f\|_L \leq 1} \mathbb{E}_{\mathbf{u} \sim \mu}[f(\mathbf{u})] - \mathbb{E}_{\mathbf{v} \sim \nu}[f(\mathbf{v})], \quad (5)$$

where $\tilde{\mathbf{x}} = g(\mathbf{x}, \mathbf{z})$, and μ and ν denote the internal distributions of patches in \mathbf{x} and $\tilde{\mathbf{x}}$, respectively. Here, $\|f\|_L$ is the Lipschitz constant of f . In practice, we introduce a gradient penalty (Gulrajani et al., 2017) to optimize Problem (5) $\mathcal{R}_{\text{gp}}(f) = \mathbb{E}[(\|\nabla f(\hat{\mathbf{x}})\| - 1)^2]$ in its dual form.

Classification loss. The classification loss $\mathcal{L}_c(g; h)$ can be defined as the distance between the prediction $g(\mathbf{x}, \mathbf{z})$ and the ground truth \mathbf{y} (untargeted attack), or the opposite of the distance between the prediction and the target class \mathbf{y}_t (targeted attack). Then, the loss $\mathcal{L}_c(g; h)$ can be written as:

$$\mathcal{L}_c(g; h) = \begin{cases} -\mathcal{L}(h(g(\mathbf{x}, \mathbf{z})), \mathbf{y}), & \text{untargeted attack,} \\ \mathcal{L}(h(g(\mathbf{x}, \mathbf{z})), \mathbf{y}_t), & \text{targeted attack.} \end{cases} \quad (6)$$

The detailed algorithm is shown in Algorithm 1.

5. Adversarial Defense with IWD

Relying on IWD, our proposed method (IWDA) is able to effectively attack the classifier by distribution perturbation on the manifold. Note that the attack and defense are coupled tasks. Essentially, with sufficient adversarial examples, we are able to learn a robust classifier. In this sense, we propose a new defense method with IWD, called IWDD.

5.1. Defense Objective Function

Mathematically, the **adversarial defense** problem aims to learn a robust classifier h to defend against the attacks from an adversarial generator g to be learned. Following (Madry et al., 2018; Shafahi et al., 2019), we can learn h and g simultaneously by solving the following minimax problem:

$$\min_h \mathbb{E}_{(\mathbf{x}, \mathbf{y}) \sim \mathcal{D}} \left[\max_g \mathcal{L}(h(\tilde{\mathbf{x}}), \mathbf{y}) \right], \text{ s.t. } \tilde{\mathbf{x}} \in \mathcal{B}_x(\mathbf{x}, \epsilon(\ell_p)). \quad (7)$$

Due to the limitations of the ℓ_p distance, these methods are limited in improving the robustness of a classifier. By contrast, IWD is able to obtain a large perturbation from Theorem 1. In this sense, we derive an upper bound to enhance the robustness of the classifier relying on IWD.

To begin with, we define the expected classification error as $\mathcal{E}_{\mathcal{D}}(h) = \mathbb{E}_{(\mathbf{x}, \mathbf{y}) \sim \mathcal{D}} [\mathbb{1}\{h(\mathbf{x}) \neq \mathbf{y}\}]$ and let $\mathcal{E}_{\mathcal{D}}^* = \inf_h \mathcal{E}_{\mathcal{D}}(h)$. Following (Zhang et al., 2019), we define the attack classification error as below.

Algorithm 1 Attack method (IWDA).

Input: A sample \mathbf{x} , the hyper-parameters λ and τ , the number of iterations of the discriminator per generator iteration n_{critic} , Adam hyper-parameters β_1, β_2 .

Output: The discriminator f , the generator g ,

```

1: while not converged do
2:   for  $t = 0, \dots, n_{\text{critic}}$  do
3:     Adversarial examples  $\tilde{\mathbf{x}} = g(\mathbf{x}, \mathbf{z})$ , where  $\mathbf{z} \sim \mathcal{N}(\mathbf{0}, \mathbf{I})$ 
4:     Sample  $\hat{\mathbf{x}} \leftarrow \rho \mathbf{x} + (1 - \rho)\tilde{\mathbf{x}}$ , where  $\rho \sim \mathcal{U}(0, 1)$ 
5:     Gradient penalty:  $\mathcal{R}_{\text{gp}}(f) = \mathbb{E}[(\|\nabla_{\hat{\mathbf{x}}} f(\hat{\mathbf{x}})\|_2 - 1)^2]$ 
6:     Update discriminator  $f$  by ascending the gradient:

```

$$\nabla_w [\hat{\mathbb{E}}_{\mathbf{u} \sim \mu}[f(\mathbf{u})] - \hat{\mathbb{E}}_{\mathbf{v} \sim \nu}[f(\mathbf{v})] + \lambda \mathcal{R}_{\text{gp}}(f)]$$

```

7:   end for
8:   Update the generator  $g$  by descending the gradient:

```

$$\nabla_v [-\hat{\mathbb{E}}_{\mathbf{v} \sim \nu} f(\mathbf{v}) + \tau \mathcal{L}_c(g; h)]$$

```

9: end while

```

Definition 4 (Attack classification error) Given a sample \mathbf{x} , if there exists an $\epsilon(d)$ -adversarial example $\tilde{\mathbf{x}} \in \mathcal{B}_x(\mathbf{x}, \epsilon(d))$ such that $h(\tilde{\mathbf{x}}) \neq \mathbf{y}$, the attack classification error of a classifier can be defined as:¹

$$\mathcal{E}_{\mathcal{B}_x}(h) = \mathbb{E}_{(\mathbf{x}, \mathbf{y}) \sim \mathcal{D}} [\mathbb{1}\{\exists \tilde{\mathbf{x}} \in \mathcal{B}_x(\mathbf{x}, \epsilon(d)), \text{ s.t. } h(\tilde{\mathbf{x}}) \neq \mathbf{y}\}].$$

Based on the definition above, we derive the following upper bound to address the robustness of the classifier.

Theorem 2 (Upper bound) Let $\mathcal{L}(h) = \mathbb{E}[\mathcal{L}(h(\mathbf{x}), \mathbf{y})]$ be the \mathcal{L} -risk of h and its optimum $\mathcal{L}^* = \inf_h \mathcal{L}(h)$. There exists a concave function $\xi(\cdot)$ on $[0, \infty)$ such that $\xi(0) = 0$ and $\xi(\delta) \rightarrow 0$ as $\delta \rightarrow 0^+$, we have the following upper bound,

$$\mathcal{E}_{\mathcal{B}_x}(h) - \mathcal{E}_{\mathcal{D}}^* \leq \xi(\mathcal{L}(h) - \mathcal{L}^*) + \mathbb{E} \left[\sup_{\tilde{\mathbf{x}} \in \mathcal{B}_x(\mathbf{x}, \epsilon(\mathcal{W}))} \mathcal{L}(h(\tilde{\mathbf{x}}), \mathbf{y}) \right].$$

From Theorem 2, we minimize the upper bound such that $\mathcal{E}_{\mathcal{B}_x}(h) - \mathcal{E}_{\mathcal{D}}^*$ can be small. In this way, the attack probability can be guaranteed to be sufficiently small. To this end, we propose a robust minimax objective function as follows.

$$\min_h \mathbb{E}_{(\mathbf{x}, \mathbf{y}) \sim \mathcal{D}} \left[\beta \mathcal{L}(h(\mathbf{x}), \mathbf{y}) + \max_{\tilde{\mathbf{x}} \in \mathcal{B}_x(\mathbf{x}, \epsilon(\mathcal{W}))} \mathcal{L}(h(\tilde{\mathbf{x}}), \mathbf{y}) \right], \quad (8)$$

where $\tilde{\mathbf{x}} = g(\mathbf{x}, \mathbf{z})$, and β is a hyper-parameter in practice. In Problem (8), the first term aims to minimize the natural classification loss between the prediction $h(\mathbf{x})$ and the ground-truth \mathbf{y} , while the second term encourages to generate $\epsilon(\mathcal{W})$ -adversarial examples. By optimizing Problem (8), the generated adversarial examples can be generated to cover the data distribution to improve the robustness of the classifier. The detailed algorithm is shown in Algorithm 2.

¹We justify the existence of $\epsilon(d)$ -adversarial examples in Supplementary materials.

5.2. Minimax Game Analysis

We analyze the generalization performance of our proposed defense method via a minimax game analysis. To begin with, we give a formal definition of the expected and empirical adversarial risk as follows.

Definition 5 (Adversarial risk) *Given a hypothesis $h \in \mathcal{H}$ and the classification boundary neighborhood $\mathcal{B}_h(h, \epsilon(\mathcal{W}))$, the expected adversarial risk can be defined as,*

$$\mathcal{R}_{\mathcal{D}}(h) = \mathbb{E}_{(\mathbf{x}, \mathbf{y}) \sim \mathcal{D}} \left[\beta \mathcal{L}(h(\mathbf{x}), \mathbf{y}) + \max_{\tilde{\mathbf{x}} \in \mathcal{B}_x(\mathbf{x}, \epsilon(\mathcal{W}))} \mathcal{L}(h(\tilde{\mathbf{x}}), \mathbf{y}) \right],$$

where \mathcal{D} is the real data distribution. We also define the empirical adversarial risk as $\mathcal{R}_{\mathcal{D}_n}(h)$ over the empirical distribution \mathcal{D}_n with n training data.

Based on this definition, we introduce a transport map (Vilani, 2008) to pushforward the distribution \mathcal{D} to a new distribution \mathcal{D}' that contains adversarial examples.

Lemma 1 (Equivalence property) *Let $\mathcal{D}' = T_{\#} \mathcal{D}$ be a pushforward of the distribution \mathcal{D} by a transport map T . For any hypothesis h , the adversarial risk is equivalent to*

$$\mathcal{R}_{\mathcal{D}}(h) = \mathbb{E}_{(\mathbf{x}, \mathbf{y}) \sim \mathcal{D}} [\beta \mathcal{L}(h(\mathbf{x}), \mathbf{y})] + \mathbb{E}_{(\mathbf{x}, \mathbf{y}) \sim \mathcal{D}'} [\mathcal{L}(h(\mathbf{x}), \mathbf{y})].$$

Based on lemma 1, the expected adversarial risk over the distribution \mathcal{D} is equivalent to the standard adversarial risk over the new distribution \mathcal{D}' . For convenience, we let $\tilde{\Psi} = \{\tilde{\psi} : (\mathbf{x}, \mathbf{y}) \rightarrow \mathcal{L}(h(\mathbf{x}), \mathbf{y}), (\mathbf{x}, \mathbf{y}) \sim \mathcal{D}\}$ and $\Psi = \{\psi : (\mathbf{x}, \mathbf{y}) \rightarrow \mathcal{L}(h(\mathbf{x}), \mathbf{y}), (\mathbf{x}, \mathbf{y}) \sim \mathcal{D}'\}$, then we derive the following generalization bound.

Theorem 3 (Generalization bound) *Given a bounded instance space $\Omega = \mathcal{X} \times \mathcal{Y}$, i.e., $\text{diam}(\Omega) < \infty$, we assume ψ is upper semi-continuous and uniformly bounded function $0 \leq \psi(\mathbf{x}) \leq M$, and a constant L exists such that ψ satisfies $\psi(\mathbf{x}') - \psi(\mathbf{x}) \leq L \|\mathbf{x} - \mathbf{x}'\|_2$ for any \mathbf{x}' . For any $\psi \in \Psi$, with $c > 0$ and the probability at least $1 - \delta$, we have*

$$\mathcal{R}_{\mathcal{D}}(h) - \mathcal{R}_{\mathcal{D}_n}(h) \leq 2\mathfrak{R}(\tilde{\Psi}) + \frac{24\mathfrak{C}(\Psi)}{\sqrt{n}} + 2M \sqrt{\frac{\log(1/\delta)}{2n}} + 24c\sqrt{\pi/n} \text{diam}(\Omega),$$

where $\mathfrak{R}(\tilde{\Psi})$ is the Rademacher complexity of $\tilde{\Psi}$, and $\mathfrak{C}(\Psi)$ is the covering number of Ψ (Sinha et al., 2018).

From Theorem 3, our proposed defense method has good generalization when the number of diverse adversarial examples is sufficiently large. In this sense, the diversity of adversarial examples is required to cover the whole data distribution to improve defense performance. In contrast, existing defense methods are limited to improve the generalization performance because of lacking diverse adversarial examples. This theoretical result coincides with that the adversarial examples are features (Ilyas et al., 2019).

Algorithm 2 Defense method (IWDD).

Input: Training data $\{\mathbf{x}_i, \mathbf{y}_i\}_{i=1}^n$, the number of epochs T , the batch size m , the hyper-parameters λ, τ, β , the number of iterations of the discriminator per generator iteration n_{critic} , Adam hyper-parameters β_1, β_2 , SGD learning rate λ_{f}

Output: The classifier h , the discriminator f , the generator g ,

1: **for** $t = 1, \dots, T$ **do**

2: Sample a mini-batch $(\mathbf{x}, \mathbf{y}) \sim \mathcal{D}_m$

3: Generate adversarial examples $\tilde{\mathbf{x}}$ using Alg. 1

4: Construct a set of adversarial examples $\tilde{\mathcal{B}}_x(\epsilon(\mathcal{W}))$

5: Update the discriminator and generator using Alg. 1

$$\nabla_{w,v} \left[-\hat{\mathbb{E}}_{\mathcal{D}_m} [\mathcal{L}(h(\tilde{\mathbf{x}}), \mathbf{y})] \right], \tilde{\mathbf{x}} \in \tilde{\mathcal{B}}_x(\mathbf{x}, \epsilon(\mathcal{W}))$$

6: Update the classifier h by descending the gradient:

$$\nabla_{\theta} \left[\hat{\mathbb{E}}_{\mathcal{D}_m} [\beta \mathcal{L}(h(\mathbf{x}), \mathbf{y}) + \mathcal{L}(h(\tilde{\mathbf{x}}), \mathbf{y})] \right]$$

7: **end for**

6. Experiments

Implementation details. We implement our method based on PyTorch (Paszke et al., 2019). During the training, we use an Adam optimizer (Kingma & Ba, 2015) to update the generator and the discriminator models with $\beta_1=0.5$ and $\beta_2=0.999$ and set the learning rate as 0.0005. Here, the architectures of two models are the same as that of (Rott Shaham et al., 2019). Additionally, we use two pre-trained classifiers (i.e., Inception-v3 (Szegedy et al., 2016) and ResNet-101 (He et al., 2016)) in the attack methods. For the defense methods, we use an SGD optimizer to train a new classifier with 200 epochs, a learning rate of 0.1, and a batch size of 128. More details of implementation and network architectures are provided in Supplementary Materials. In addition, we compare our attack method with FGSM (Goodfellow et al., 2014), ADef (Alaifari et al., 2019), EOT (Athalye et al., 2018) and stAdv (Xiao et al., 2018). For defense methods, we use free-PGD (Shafahi et al., 2019) and PGD (Madry et al., 2018) as baseline methods.

Dataset. We conduct experiments on ImageNet (Russakovsky et al., 2015). In addition, we arbitrarily choose 10 classes from ImageNet (called tiny ImageNet), e.g., barn, megalith, alp, cliff, coral reef, lakeside, seashore, valley, volcano, and coral fungus. There are 1300 images for training and 50 images for validation in each class.

Evaluation metrics. For attack, we use attack success rate (ASR) (Goodfellow et al., 2014) to measure the probability of successfully attacking the pre-trained classifier. For defense, we calculate the classification accuracy on clean samples and adversarial examples.

6.1. Attack Results on ImageNet

In this experiment, we consider Inception-v3 and ResNet-101 as classifiers trained by naturally training and the free-

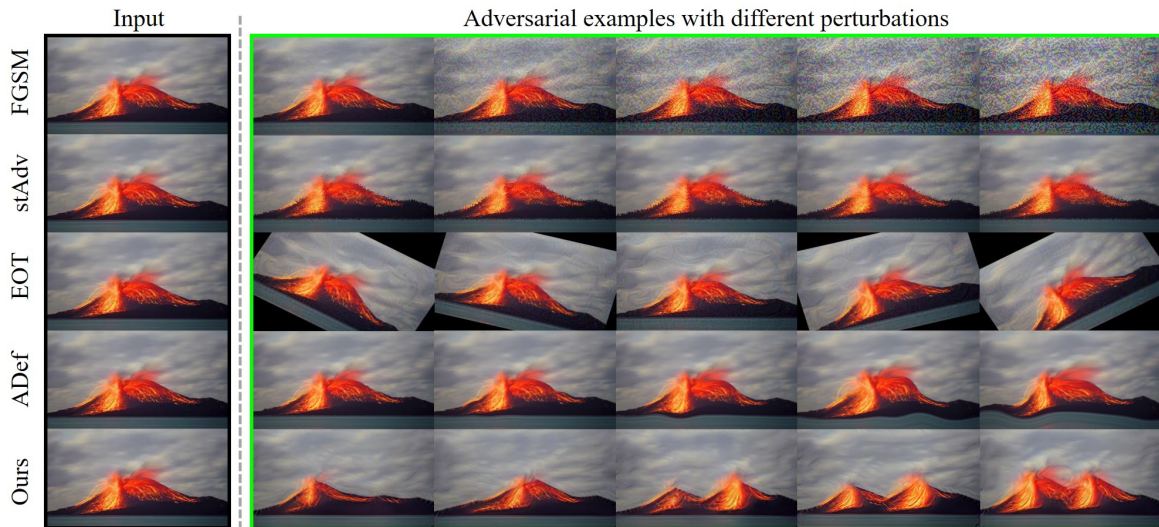


Figure 4. Comparisons of generated untargeted adversarial examples with different intensities of perturbation. (FGSM: step size; stAdv: flow; EOT: rotations; ADef: smoothness; Ours: internal Wasserstein distance)

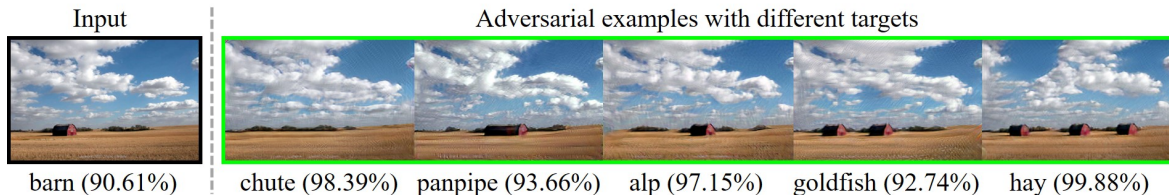


Figure 5. Generated targeted adversarial examples with different targets.

Table 1. Comparisons of attack success rate for different attack methods on ImageNet (3-6 lines: untargeted; 7-8 lines: targeted).

Model	Attack success rate (ASR) (%)				
	FGSM	stAdv	EOT	ADef	IWDA
Inception-v3	69.78	99.45	99.73	100.00	100.00
Inception-v3 (free-PGD)	15.51	69.31	88.12	97.36	100.00
ResNet-101	89.43	99.73	99.46	100.00	100.00
ResNet-101 (free-PGD)	18.83	61.42	91.12	97.22	100.00
Inception-v3 (targeted)	0.27	18.96	48.63	55.77	90.66
ResNet-101 (targeted)	1.90	59.35	79.13	87.26	94.58

PGD method on ImageNet. Note that we use free-PGD instead of PGD since PGD is inefficient when training on ImageNet (Shafahi et al., 2019). First, we perform untargeted attacks on pre-trained classifiers and evaluate the performance on the validation set of tiny ImageNet.

Quantitative comparison. From Table 1, IWDA achieves the highest ASR than other baseline methods. It suggests that IWDA is able to generate effective adversarial examples by finding larger perturbations relying on the internal Wasserstein distance. In contrast, FGSM and EOT perturb the image with gradient updates and thus the perturbation

is insufficient to confuse the classifier. In addition, stAdv and ADef apply pixel based transformation to improve ASR. However, when attacking a robust model like free-PGD, these methods are difficult to achieve good ASR results since their transformation (*e.g.*, perturbation or distortion) fail to result in large perturbation in the Euclidean space.

Qualitative comparison. We compare different attack methods that generate adversarial examples with different intensities of perturbation in Figure 4. Besides, we measure the distance between an original image and the corresponding adversarial examples in Supplementary Materials.

In Figure 4, IWDA is able to generate diverse adversarial examples by exploiting the internal distribution of the input image. These samples are far away from the input image and hence cause the large perturbation. Moreover, they are realistic and semantically invariant for human understanding. In this sense, IWDA has good generalization to generate diverse adversarial examples and helps the classifier to understand a real-world image from different views. In contrast, the baseline methods lack diversity when using a large perturbation to the images. For example, FGSM often destroys the image resolution when setting a large step

Table 2. Accuracy (%) of robust models on the validation set of tiny ImageNet. (“natural” training uses only clean data while others use both training data and generated adversarial examples.)

Model	Training method	Clean data	PGD-10
Inception-v3	natural	83.00	0.00
	free-PGD	62.80	28.40
	PGD	70.60	45.00
	IWDD	70.80	46.00
ResNet-101	natural	79.80	0.00
	free-PGD	41.40	24.20
	PGD	69.80	44.80
	IWDD	71.00	46.00

size, and EOT keeps the adversarial the same as the original image but changes different rotations. In addition, stAdv damages the smoothness of edges of objects by strengthening the flow of the image, while ADef maintains the smoothness of the image but deforms the original image.

Targeted attack. We also conduct targeted attack on ImageNet in Table 1. In addition, we demonstrate the effect of choosing different target labels for a given image in Figure 5. Our method is able to generate target-specified adversarial examples to confuse the classifier with high probability. Moreover, the adversarial examples contain one or more houses with different sizes, shapes and locations.

6.2. Comparisons of Perturbation

We further compare the perturbation distance of different methods. Under the untargeted attack setting, we use pre-trained ResNet-101 to generate adversarial examples on the validation set of tiny ImageNet. Specifically, we measure three metrics (*i.e.*, ℓ_2 , ℓ_∞ and IWD) between an original sample and its corresponding adversarial example. We plot histograms to count the number of perturbed samples over three metrics in Figure 6. IWDA is able to results in large perturbation and thus achieves the highest average of the ℓ_2 and ℓ_∞ distance compared to baseline methods. Moreover, IWDA achieves the smallest IWD values compared to other baseline methods. This suggests that IWDA is able to perturb an image far away to generate adversarial examples which are still realistic and diverse. In addition, we provide more experimental results in Supplementary Materials.

6.3. Defense Results on Tiny ImageNet

In this experiment, we use Inception-v3 and ResNet-101 to demonstrate the effectiveness of IWDD. Due to the inefficiency of PGD (Shafahi et al., 2019), we train all defense methods on tiny ImageNet. Specifically, we calculate the top-1 accuracy on the validation set of tiny ImageNet (clean data) and the adversarial examples generated by PGD with 10 iterations (PGD-10), respectively.

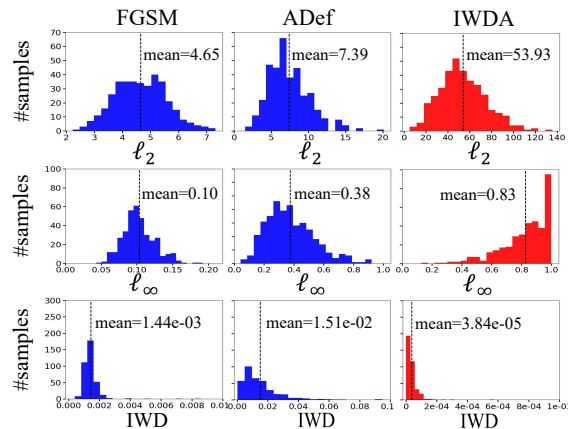


Figure 6. Comparisons of the perturbation for different methods. We use the ℓ_2 distance, the ℓ_∞ distance and IWD to measure the similarity between the original samples and perturbed samples.

In Table 2, IWDD is robust to the adversarial examples generated by PGD-10 and achieves the best results than other defense methods. From these results, we justify that diverse adversarial examples are required in the adversarial learning. Therefore, our proposed defense method is able to improve the robustness of the classifier relying on IWD. In contrast, free-PGD and PGD methods are limited to improve the generalization performance on PGD-10 adversarial examples.

6.4. Ablation Study

In this experiment, we evaluate the influences of the hyperparameters τ and β in the attack and defense method. By setting different values of τ and β , we attack the pre-trained ResNet-101, and train a new ResNet-101 on tiny ImageNet. The attack success rate and validation accuracy are provided in Supplementary Materials. When setting $\tau=0.1$, IWDA achieves the highest ASR score and best qualitative results. The performance improves with the increase of τ . Moreover, IWDD obtains the best performance with $\beta=0.1$ when fixing $\tau=0.1$. Thus, we set $\tau=0.1$ and $\beta=0.1$ in practice.

7. Conclusion

In this paper, we have proposed an internal Wasserstein distance (IWD) to exploit the internal distribution of the data for both attack and defense methods. Relying on IWD, we propose a novel attack method to generate diverse adversarial examples. Meanwhile, we derive an upper bound and propose a new defense method to improve the robustness of the classifier. Extensive experiments on ImageNet demonstrate the effectiveness of both attack and defense methods. Moreover, we analyze the generalization performance of our defense method and prove that robustness requires more diverse adversarial examples in the adversarial training.

Acknowledgements. This work was partially supported by Key-Area Research and Development Program of Guangdong Province (2018B010107001, 2019B010155002, 2019B010155001), National Natural Science Foundation of China (NSFC) 61836003 (key project), National Natural Science Foundation of China (NSFC) 62072190, 2017ZT07X183, Tencent AI Lab Rhino-Bird Focused Research Program (No.JR201902), Fundamental Research Funds for the Central Universities D2191240.

References

- Alaifari, R., Alberti, G. S., and Gauksson, T. ADef: an iterative algorithm to construct adversarial deformations. In *International Conference on Learning Representations*, 2019.
- Alt, H. Lineare funktionalanalysis. eine anwendungsorientierte einführung.. aufl. Springer-Verlag, 10:978–3, 2006.
- Arjovsky, M., Chintala, S., and Bottou, L. Wasserstein generative adversarial networks. In *International Conference on Machine Learning*, pp. 214–223, 2017.
- Athalye, A., Engstrom, L., Ilyas, A., and Kwok, K. Synthesizing robust adversarial examples. In *Proceedings of the 35th International Conference on Machine Learning*, pp. 284–293, 2018.
- Croce, F. and Hein, M. Minimally distorted adversarial examples with a fast adaptive boundary attack. In *International Conference on Machine Learning*, 2020.
- Dai, H., Li, H., Tian, T., Huang, X., Wang, L., Zhu, J., and Song, L. Adversarial attack on graph structured data. In *Proceedings of the 35th International Conference on Machine Learning*, pp. 1115–1124, 2018.
- Goodfellow, I. J., Shlens, J., and Szegedy, C. Explaining and harnessing adversarial examples. In *International Conference on Learning Representations*, 2014.
- Gulrajani, I., Ahmed, F., Arjovsky, M., Dumoulin, V., and Courville, A. C. Improved training of wasserstein gans. In *Advances in Neural Information Processing Systems*, pp. 5767–5777, 2017.
- He, K., Zhang, X., Ren, S., and Sun, J. Deep residual learning for image recognition. In *The IEEE Conference on Computer Vision and Pattern Recognition*, 2016.
- Ilyas, A., Santurkar, S., Tsipras, D., Engstrom, L., Tran, B., and Madry, A. Adversarial examples are not bugs, they are features. *arXiv preprint arXiv:1905.02175*, 2019.
- Kannan, H., Kurakin, A., and Goodfellow, I. Adversarial logit pairing. *arXiv preprint arXiv:1803.06373*, 2018.
- Kingma, D. P. and Ba, J. Adam: A method for stochastic optimization. In *International Conference on Learning Representations*, 2015.
- Larsen, A. B. L., Sønderby, S. K., Larochelle, H., and Winther, O. Autoencoding beyond pixels using a learned similarity metric. In *Proceedings of the 33th International Conference on Machine Learning*, pp. 1558–1566, 2016.
- Liu, H.-T. D., Tao, M., Li, C.-L., Nowrouzezahrai, D., and Jacobson, A. Beyond pixel norm-balls: Parametric adversaries using an analytically differentiable renderer. In *International Conference on Learning Representations*, 2019.
- Madry, A., Makelov, A., Schmidt, L., Tsipras, D., and Vladu, A. Towards deep learning models resistant to adversarial attacks. In *International Conference on Learning Representations*, 2018.
- Pang, T., Du, C., Dong, Y., and Zhu, J. Towards robust detection of adversarial examples. In *Advances in Neural Information Processing Systems*, 2018.
- Paszke, A., Gross, S., Massa, F., Lerer, A., Bradbury, J., Chanan, G., Killeen, T., Lin, Z., Gimelshein, N., Antiga, L., Desmaison, A., Köpf, A., Yang, E., DeVito, Z., Raison, M., Tejani, A., Chilamkurthy, S., Steiner, B., Fang, L., Bai, J., and Chintala, S. Pytorch: An imperative style, high-performance deep learning library. In *Advances in Neural Information Processing Systems*, pp. 8024–8035, 2019.
- Raghunathan, A., Xie, S. M., Yang, F., Duchi, J. C., and Liang, P. Understanding and mitigating the tradeoff between robustness and accuracy. In *International Conference on Machine Learning*, 2020.
- Rice, L., Wong, E., and Kolter, J. Z. Overfitting in adversarially robust deep learning. *arXiv preprint arXiv:2002.11569*, 2020.
- Ronneberger, O., Fischer, P., and Brox, T. U-net: Convolutional networks for biomedical image segmentation. In *International Conference on Medical image computing and computer-assisted intervention*, pp. 234–241, 2015.
- Rott Shaham, T., Dekel, T., and Michaeli, T. Singan: Learning a generative model from a single natural image. In *The IEEE International Conference on Computer Vision*, 2019.
- Roweis, S. T. and Saul, L. K. Nonlinear dimensionality reduction by locally linear embedding. *science*, 290(5500): 2323–2326, 2000.

- Russakovsky, O., Deng, J., Su, H., Krause, J., Satheesh, S., Ma, S., Huang, Z., Karpathy, A., Khosla, A., Bernstein, M., Berg, A. C., and Fei-Fei, L. ImageNet Large Scale Visual Recognition Challenge. *International Journal of Computer Vision*, 115(3):211–252, 2015.
- Shafahi, A., Najibi, M., Ghiasi, A., Xu, Z., Dickerson, J., Studer, C., Davis, L. S., Taylor, G., and Goldstein, T. Adversarial training for free! In *Advances in Neural Information Processing Systems*, 2019.
- Sinha, A., Namkoong, H., and Duchi, J. Certifiable distributional robustness with principled adversarial training. In *International Conference on Learning Representations*, 2018.
- Szegedy, C., Zaremba, W., Sutskever, I., Bruna, J., Erhan, D., Goodfellow, I., and Fergus, R. Intriguing properties of neural networks. In *International Conference on Learning Representations*, 2014.
- Szegedy, C., Vanhoucke, V., Ioffe, S., Shlens, J., and Wojna, Z. Rethinking the inception architecture for computer vision. In *The IEEE Conference on Computer Vision and Pattern Recognition*, pp. 2818–2826, 2016.
- Tenenbaum, J. B., De Silva, V., and Langford, J. C. A global geometric framework for nonlinear dimensionality reduction. *science*, 290(5500):2319–2323, 2000.
- Tsipras, D., Santurkar, S., Engstrom, L., Turner, A., and Madry, A. Robustness may be at odds with accuracy. In *International Conference on Learning Representations*, 2019.
- Villani, C. *Optimal transport: old and new*, volume 338. Springer Science & Business Media, 2008.
- Xiao, C., Zhu, J.-Y., Li, B., He, W., Liu, M., and Song, D. Spatially transformed adversarial examples. In *International Conference on Learning Representations*, 2018.
- Xu, K., Liu, S., Zhao, P., Chen, P.-Y., Zhang, H., Fan, Q., Erdogmus, D., Wang, Y., and Lin, X. Structured adversarial attack: Towards general implementation and better interpretability. In *International Conference on Learning Representations*, 2019.
- Yang, Y.-Y., Rashtchian, C., Zhang, H., Salakhutdinov, R., and Chaudhuri, K. A Closer Look at Accuracy vs. Robustness. In *Advances in Neural Information Processing Systems*, 2020.
- Zhang, H., Yu, Y., Jiao, J., Xing, E. P., Ghaoui, L. E., and Jordan, M. I. Theoretically principled trade-off between robustness and accuracy. In *International Conference on Machine Learning*, 2019.
- Zhang, J., Xu, X., Han, B., Niu, G., Cui, L., Sugiyama, M., and Kankanhalli, M. Attacks which do not kill training make adversarial learning stronger. In *International Conference on Machine Learning*, 2020.
- Zhao, Z., Dua, D., and Singh, S. Generating natural adversarial examples. In *International Conference on Learning Representations*, 2018.